

Efficient Non-parametric Bayesian Hawkes Processes

Rui Zhang^{1,2}, Christian Walder^{1,2}, Marian-Andrei Rizoiu³ and Lexing Xie^{1,2}

¹The Australian National University, Australia

²Data61 CSIRO, Australia

³University of Technology Sydney, Australia

{firstname}. {lastname}@[anu.edu.au¹, data61.csiro.au², uts.edu.au³]

Abstract

In this paper, we develop an efficient non-parametric Bayesian estimation of the kernel function of Hawkes processes. The non-parametric Bayesian approach is important because it provides flexible Hawkes kernels and quantifies their uncertainty. Our method is based on the cluster representation of Hawkes processes. Utilizing the finite support assumption of the Hawkes process, we efficiently sample random branching structures and thus, we split the Hawkes process into clusters of Poisson processes. We derive two algorithms — a block Gibbs sampler and a maximum a posteriori estimator based on expectation maximization — and we show that our methods have a linear time complexity, both theoretically and empirically. On synthetic data, we show our methods to be able to infer flexible Hawkes triggering kernels. On two large-scale Twitter diffusion datasets, we show that our methods outperform the current state-of-the-art in goodness-of-fit and that the time complexity is linear in the size of the dataset. We also observe that on diffusions related to online videos, the learned kernels reflect the perceived longevity for different content types such as music or pets videos.

1 Introduction

The Hawkes process [Hawkes, 1971] is a useful model of self-exciting point data in which the occurrence of a point increases the likelihood of arrival of new points. More specifically, every point causes the conditional intensity function λ — which modulates the arrival rate of new points — to increase. An alternative representation of the Hawkes process is a cluster of Poisson processes [Hawkes and Oakes, 1974], which categorizes points into *immigrants* and *offspring*. Immigrant points are generated independently at a background rate μ ; offspring points are triggered by existing points at a rate of ϕ . Points can therefore be structured into clusters, where each cluster contains a point and the offspring it directly generated. This leads to a tree structure, also known as the branching structure (an example is shown in Fig. 1).

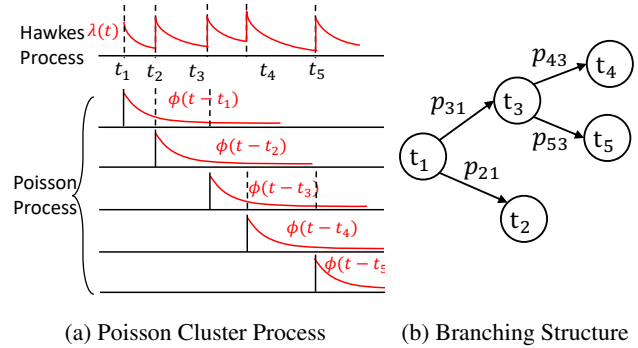


Figure 1: The cluster Representation of a Hawkes Process. (a) A Hawkes process with decaying triggering kernel $\phi(\cdot)$ has intensity $\lambda(t)$ which increases after each new point is generated. It can be represented as a cluster of Poisson processes $PP(\phi(t - t_i))$ associated with each t_i . (b) The branching structure corresponding to the triggering relationships shown in (a), where an edge $t_i \rightarrow t_j$ means that t_i triggered t_j with the probability p_{ji} (calculated as Eq. (9)).

1.1 Background and Motivations.

ϕ is important as it is shared and decides the class of the whole process and recently the Hawkes process with various ϕ has been studied. Mishra *et al.* [2016] employ the branching factor of the Hawkes process with the power-law kernel to predict popularity of tweets; Kurashima *et al.* [2018] predict human actions using a Hawkes process equipped with exponential, Weibull and Gaussian mixture kernels; online popularity unpredictability is explained using the Hawkes process with a variant of the exponential kernel by Rizoiu *et al.* [2018]. However, most work employes Hawkes process with parametric kernels, which encodes strong assumptions, and limits the expressivity of the model. Can we design a practical approach to learn flexible representations of the optimal Hawkes kernel function ϕ from data?

A typical solution is the non-parametric estimation of the kernel function [Lewis and Mohler, 2011; Zhou *et al.*, 2013b; Bacry and Muzy, 2014]. These are all frequentist methods which do not quantify the uncertainty of the learned kernels. There exists work [Rasmussen, 2013; Linderman and Adams, 2015] on the Bayesian inference for the Hawkes process. To scale past toy-dataset sizes these methods require either parametric triggering kernels or discretization of the

Methods	Time Complexity	Bayesian	Continuous	Non-parametric
Zhou <i>et al.</i> [2013a]	$O(n^3)$	×	✓	×
Xu <i>et al.</i> [2016]	$O(n^3)$	×	✓	×
Lewis and Mohler [2011]	$O(n^3)$	×	×	✓
Zhou <i>et al.</i> [2013b]	$O(n^3)$	×	×	✓
Rasmussen [2013]	$O(n)$	✓	✓	×
Linderman and Adams [2015]	$O(n)$	✓	interval-censored	×
Donnet <i>et al.</i> [2018]	unspecified	✓	✓	✓
Ours	$O(n)$	✓	✓	✓

Table 1: Related Works on Non-parametric Hawkes Processes.

input domain, which in turn leads to poor scaling with the dimension of the domain and sensitivity to the choice of discretization. The work closest to our own is that of Donnet *et al.* [2018], however their main contributions are theoretical; on the practical side they resort to an unscalable Markov chain Monte Carlo (MCMC) estimator. We comparatively summarize related works in Table 1. To the best of our knowledge, our work is the first work proposing a Bayesian non-parametric Hawkes process estimation procedure, with a linear time complexity allowing it to be applied to real-world datasets, and without requiring discretization of domains.

1.2 Contributions.

In this paper, we propose a general framework for the efficient non-parametric Bayesian inference of Hawkes processes.

(1) We exploit block Gibbs sampling [Ishwaran and James, 2001] to iteratively sample the latent branching structure, the background intensity μ and the triggering kernel ϕ . In each iteration, the point data are decomposed as a cluster of Poisson processes based on the sampled branching structure. This is exemplified in Fig. 1, in which a Hawkes process (shown on the top temporal axis of Fig. 1a) is decomposed into several Poisson processes (the following temporal axes); the corresponding branching structure is shown in Fig. 1b. The posterior μ and ϕ are estimated using the resulting cluster processes. Our framework is close to the stochastic Expectation-Maximization (EM) algorithm [Celeux and Diebolt, 1985] where posterior μ and ϕ are estimated [Lloyd *et al.*, 2015; Walder and Bishop, 2017] in the M-step and random samples of μ and ϕ are drawn. We adapt the approach of the recent non-parametric Bayesian estimation for Poisson process intensities, termed Laplace Bayesian Poisson process (LBPP) [Walder and Bishop, 2017], to estimate the posterior ϕ given the sampled branching structure.

(2) We utilize the finite support assumption of the Hawkes Process to speed up sampling and computing the probability of the branching structure. We theoretically show our method to be of linear time complexity. Furthermore, we explore the connection with the EM algorithm [Dempster *et al.*, 1977] and develop a second variant of our method, as an approximate EM algorithm.

(3) We empirically show our method enjoys linear time complexity and can infer known analytical kernels, i.e., exponential and sinusoidal kernels. On two large-scale social media datasets, our method outperforms the current state-of-

the-art non-parametric approaches and the learned kernels reflect the perceived longevity for different content types.

2 Preliminaries

In this section, we introduce the prerequisites of our work: the Hawkes process and LBPP.

2.1 The Hawkes Process

Introduced in Section 1, the Hawkes process [Hawkes, 1971] can be specified using the conditional intensity function λ which modulates the arrival rate of points. Mathematically, conditioned on a set of points $\{t_i\}_{i=1}^N$, the intensity λ is expressed as:

$$\lambda(t) = \mu + \sum_{t_i < t} \phi(t - t_i), \quad (1)$$

where $\mu > 0$, considered as a constant, and $\phi(\cdot) : \mathbb{R} \rightarrow [0, \infty)$ are the background immigrant intensity and the triggering kernel. The log-likelihood of $\{t_i\}_{i=1}^N$ given μ and $\phi(\cdot)$ is [Rubin, 1972]:

$$\log p(\{t_i\}_{i=1}^N | \mu, \phi(\cdot)) = \sum_{i=1}^N \log \lambda(t_i) - \int_{\Omega} \lambda(t) dt, \quad (2)$$

where Ω is the sampling domain of $\{t_i\}_{i=1}^N$.

2.2 Laplace Bayesian Poisson Process (LBPP)

LBPP [Walder and Bishop, 2017] has been proposed for the non-parametric Bayesian estimation of the intensity of a Poisson process. To satisfy non-negativity of the intensity function, LBPP models the intensity function λ as a permanent process [Shirai and Takahashi, 2003], i.e., $\lambda = g \circ f$ where the link function $g(z) = z^2/2$ and $f(\cdot)$ obeys a Gaussian process (GP) prior. Alternative link functions include $\exp(\cdot)$ [Møller *et al.*, 1998; Diggle *et al.*, 2013] and $g(z) = \lambda^*(1 + \exp(-z))^{-1}$ [Adams *et al.*, 2009] where λ^* is constant.

The choice $g(z) = z^2/2$ has the analytical advantages; for some covariances the log-likelihood can be computed in closed form [Lloyd *et al.*, 2015; Flaxman *et al.*, 2017]. LBPP exploits the Mercer expansion [Mercer, 1909] of the GP covariance function $k(x, y) \equiv \text{Cov}(f(x), f(y))$,

$$k(x, y) = \sum_{i=1}^K \lambda_i e_i(x) e_i(y), \quad (3)$$

where for non-degenerate kernels, $K = \infty$. The eigenfunctions $\{e_i(\cdot)\}_i$ are chosen to be orthonormal in $L^2(\Omega, m)$ for some sample space Ω with measure m . $f(\cdot)$ can be represented as a linear combination of $e_i(\cdot)$ [Rasmussen and Williams, 2005, section 2.2], $f(\cdot) = \omega^T e(\cdot)$, and ω has a Gaussian prior, i.e., $\omega \sim \mathcal{N}(0, \Lambda)$ where $\Lambda = \text{diag}(\lambda_1, \lambda_2, \dots, \lambda_K)$ is a diagonal covariance matrix and $e(\cdot) = [e_1(\cdot), \dots, e_K(\cdot)]^T$ is a vector of basis functions. Computing the posterior distribution of the intensity function $\lambda(\cdot)$ is equivalent to estimating the posterior distribution of ω which, in LBPP, is approximated by a normal distribution (a.k.a Laplace approximation [Rasmussen and Williams, 2005, section 3.4]), i.e.,

$$\log p(\omega|X, \Omega, k) \approx \log \mathcal{N}(\omega|\hat{\omega}, Q), \quad (4)$$

where $X \equiv \{t_i\}_{i=1}^N$ is a set of point data, Ω the sample space and k the Gaussian process kernel function. $\hat{\omega}$ is selected as the mode of the true posterior and Q the negative inverse Hessian of the true posterior at $\hat{\omega}$:

$$\hat{\omega} = \underset{\omega}{\text{argmax}} \log p(\omega|X, \Omega, k), \quad (5)$$

$$Q^{-1} = -\partial_{\omega\omega^T} \log p(\omega|X, \Omega, k)|_{\omega=\hat{\omega}}. \quad (6)$$

The approximate posterior distribution of $f(t)$ is a normal distribution [Rasmussen and Williams, 2005, section 2.2]:

$$f(t) \sim \mathcal{N}(\hat{\omega}^T e(t), e(t)^T Q e(t)) \equiv \mathcal{N}(\nu, \sigma^2). \quad (7)$$

Furthermore, the posterior of $\lambda(t)$ is a Gamma distribution:

$$\text{Gamma}(x|\alpha, \beta) \equiv \beta^\alpha x^{\alpha-1} e^{-\beta x} / \Gamma(\alpha), \quad (8)$$

where $\alpha = (\nu^2 + \sigma^2)^2 / (4\nu^2\sigma^2 + 2\sigma^4)$ and $\beta = (\nu^2 + \sigma^2) / (2\nu^2\sigma^2 + \sigma^4)$.

3 Inference via Sampling

We now detail our efficient non-parametric Bayesian estimation algorithm, which samples the posterior of μ (constant background intensity) and $\phi(\cdot)$ (the triggering kernel). Our method starts with random $\mu_0, \phi_0(\cdot)$ and iterates by cycling through the following four steps (k is the iteration index):

- i Calculate $p(\mathcal{B}|X, \phi_{k-1}, \mu_{k-1})$, the distribution of the branching structure \mathcal{B} given the data X , triggering kernel ϕ_{k-1} , and background intensity μ_{k-1} (see Section 3.1).
- ii Sample a \mathcal{B}_k as per $p(\mathcal{B}|X, \phi_{k-1}, \mu_{k-1})$ (see Section 3.1).
- iii Estimate $p(\phi|\mathcal{B}_k, X)$ (Section 3.3) and $p(\mu|\mathcal{B}_k, X)$ (Section 3.2).
- iv Sample a $\phi_k(\cdot)$ and μ_k from $p(\phi(\cdot)|\mathcal{B}_k, X)$ and $p(\mu|\mathcal{B}_k, X)$, respectively.

By standard Gibbs sampling arguments, the samples of $\phi(\cdot)$ and μ drawn in the step (iv) converge to the desired posterior, modulo the Laplace approximation in (iii). As the method is based on block Gibbs sampling [Ishwaran and James, 2001], we term it *Gibbs-Hawkes*.

3.1 Distribution and Sampling of the Branching Structure

The branching structure \mathcal{B} has a data structure of tree (as Fig. 1(b)) and consists of independent triggering events.

Thus, the probability of the branching structure \mathcal{B} is the product of probabilities of triggering events, i.e., $p(\mathcal{B}) = \prod_{i=1}^N p_{ij_i}$ where p_{ij_i} is the probability of t_{j_i} triggering t_i . Given μ and $\phi(\cdot)$, p_{ij} is the ratio between $\phi(t_i - t_j)$ and $\lambda(t_i)$ (see e.g. [Lewis and Mohler, 2011]):

$$p_{ij} \equiv \phi(t_i - t_j) / \lambda(t_i), \quad j \geq 1. \quad (9)$$

Similarly, the probability of point t_i being from μ is:

$$p_{i0} \equiv \mu / \lambda(t_i). \quad (10)$$

Given these probabilities we may sample a branching structure by sampling a parent for each t_i according to probabilities $\{p_{ij}\}_{j \geq 0}$. The sampled branching structure separates a set of points into immigrants and offspring (introduced in Section 1). Immigrants can be regarded as a sequence generated from $\text{PP}(\mu)$, where $\text{PP}(\mu)$ is a Poisson process which has an intensity μ , and used to estimate the posterior μ .

The key property which we exploit in the subsequent Section 3.2 and Section 3.3 is the following. Denote by $\{t_k^{(i)}\}_{k=1}^{N_{t_i}}$, the N_{t_i} offspring generated by point t_i . If such a sequence is *aligned* to an origin at t_i , yielding $S_{t_i} \equiv \{t_k^{(i)} - t_i\}_{k=1}^{N_{t_i}}$, then the aligned sequence is drawn from $\text{PP}(\phi(\cdot))$ over $[0, T - t_i]$ where $[0, T]$ is the sample domain of the Hawkes process. The posterior distribution of $\phi(\cdot)$ is estimated on all such aligned sequences.

3.2 Posterior Distribution of μ

Continuing from the observations in Section 3.1, note that if we are given a set of points $\{t_i\}_{i=1}^M$ generated by $\text{PP}(\mu)$ over $\Omega = [0, T]$, the likelihood for $\{t_i\}_{i=1}^M$ is the Poisson likelihood, $p(\{t_i\}_{i=1}^M | \mu, \Omega) = e^{-\mu T} (\mu T)^M / M!$. For simplicity, we place a conjugate (Gamma) prior on μT , $\mu T \sim \text{Gamma}(\alpha, \beta)$; the Gamma-Poisson conjugate family conveniently gives the posterior distribution of μT , i.e., $p(\mu T | \{t_i\}_{i=1}^M, \alpha, \beta) = \text{Gamma}(\alpha + M, \beta + 1)$. We choose the scale α and the rate β in the Gamma prior by making the mean of the Gamma posterior equal to M and the variance $M/2$, which is easily shown to correspond to $\alpha = M$ and $\beta = 1$. Finally, due to conjugacy we obtain the posterior

$$p(\mu | \{t_i\}_{i=1}^M, \alpha, \beta) = \text{Gamma}(2M, 2T). \quad (11)$$

3.3 Posterior Distribution of ϕ

We handle the posterior distribution of the triggering kernel $\phi(\cdot)$ given the branching structure in an analogous manner to the LBPP method of Walder and Bishop [2017]. That is, we assume that $\phi(\cdot) = f^2(\cdot)/2$ where $f(\cdot)$ is Gaussian process distributed as described in Section 2.2. In line with [Walder and Bishop, 2017], we consider the sample domain $[0, \pi]$ and the so-called *cosine kernel*,

$$k(x, y) = \sum_{\gamma \geq 0} \lambda_\gamma e_\gamma(x) e_\gamma(y), \quad (12)$$

$$\lambda_\gamma \equiv 1 / (a(\gamma^2)^m + b), \quad (13)$$

$$e_\gamma(x) \equiv (2/\pi)^{1/2} \sqrt{1/2}^{[\gamma=0]} \cos(\gamma x). \quad (14)$$

Here, γ is a multi-index with non-negative (integral) values, $[\cdot]$ is the indicator function, a and b are parameters controlling the prior smoothness, and we let $m = 2$. This basis is orthonormal w.r.t. the Lebesgue measure on $\Omega = [0, \pi]$. The

expansion Eq. (12) is an explicit kernel construction based on the Mercer expansion as per Eq. (3), but other kernels may be used, for example by Nyström approximation of the Mercer decomposition [Flaxman *et al.*, 2017].

As mentioned at the end of Section 3.1, by conditioning on the branching structure we may estimate $\phi(\cdot)$ by considering the *aligned* sequences. In particular, letting S_{t_i} denote the aligned sequence generated by t_i , the joint distribution of ω and $\{S_{t_i}\}_{i=1}^N$ is calculated as [Walder and Bishop, 2017]

$$\begin{aligned} & \log p(\omega, \{S_{t_i}\}_{i=1}^N | \Omega, k) \\ &= \sum_{i=1}^N \sum_{\Delta t \in S_{t_i}} \log \frac{1}{2} \left(\omega^T \mathbf{e}(\Delta t) \right)^2 - \frac{1}{2} \omega^T (A + \Lambda^{-1}) \omega + C, \quad (15) \\ & A \equiv \sum_{i=1}^N \int_0^{T-t_i} \mathbf{e}(t) \mathbf{e}(t)^T dt, \quad C \equiv -\frac{1}{2} \log \left[(2\pi)^K |\Lambda| \right]. \end{aligned}$$

where K is the number of eigenfunctions. Note that there is a subtle but important difference between the integral term above and that of Walder and Bishop [2017], namely the limit of integration; closed-form expressions for the present case are provided in Appendix A. Putting the above equation into Eq. (5) and Eq. (6), and we obtain the mean $\hat{\omega}$ and the covariance Q of the (Laplace) approximate log-posterior in ω :

$$\hat{\omega} = \underset{\omega}{\operatorname{argmax}} \log p(\omega, \{S_{t_i}\}_{i=1}^N | \Omega, k), \quad (16)$$

$$Q^{-1} = - \sum_{i=1}^N \sum_{\Delta t \in S_{t_i}} 2 \mathbf{e}(\Delta t) \mathbf{e}(\Delta t)^T / (\hat{\omega}^T \mathbf{e}(\Delta t))^2 + A + \Lambda^{-1}. \quad (17)$$

Then, the posterior ϕ is achieved by Eqs. (7) and (8).

3.4 Computational Complexity

For LBPP, constructing Eq. (15) and Eq. (17) takes $O(N_o K^2)$ where K is the number of basis functions and N_o is the number of offspring. Optimizing ω (Eq. (16)) is a concave problem, which can be solved efficiently. If L-BFGS is used, $O(CK)$ will be taken to calculate the gradient on each ω where C is the number of steps stored in memory. Computing Q requires inverting a $K \times K$ matrix, which is $O(K^3)$. As a result, the complexity of estimating $p(\phi|B)$ is $O((N_o + K)K^2)$. In terms of estimating $p(\mu|B)$ taking $O(1)$, the complexity of estimating $p(\mu|B)$, $p(\phi|B)$ is linear to the number of data. The time taken to sample μ and ϕ is minor ($O(1)$ and $O(K)$ respectively), so estimation time dominates. While the naive complexity for p_{ij} is $O(N^2)$, Halpin [2013] provides an optimized approach to reduce it to $O(N)$, which relies on the finite support assumption of Hawkes processes.

The finite support assumption says that the value of the triggering kernel is negligible when the input is large [Halpin, 2013, p. 9]. As a result, the step of sampling branching structures can also be run in $O(N)$ and points with negligible impacts on another point are not sampled as its parents. Interestingly, in comparison with LBPP, while our model is in some sense more complex, it enjoys a more favorable computational complexity. In summary, we have the following complexities per iteration and in Section 5, we validate the complexity on both synthetic and real data.

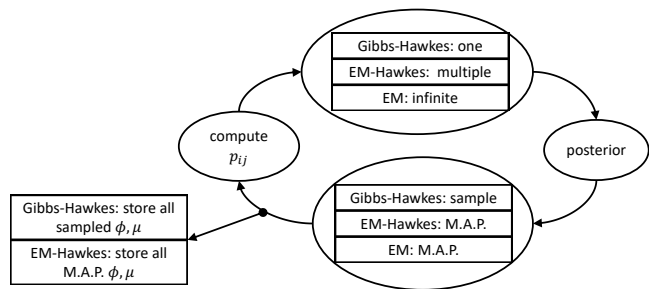


Figure 2: A visual summary of the Gibbs-Hawkes, EM-Hawkes and the EM algorithms. The differences between them are (1) the number of sampled branching structures and (2) selected ϕ and μ for p_{ij} . In contrast with with Gibbs-Hawkes, the EM-Hawkes method draws multiple branching structures at once and calculates p_{ij} using M.A.P. ϕ and μ . The EM algorithm is equivalent to sampling infinite branching structures and exploiting M.A.P. or constrained M.L.E. ϕ and μ to calculate p_{ij} (see Section 4).

4 Maximum-A-Posterior Estimation

We explore a connection between the sampler of section 3 and the EM algorithm, which allows us to introduce an analogous but intermediate scheme between them. In contrast to the random sampler of Section 3, the proposed scheme employs a deterministic *maximum-a-posteriori* (M.A.P.) sampler.

Relationship to EM. In Section 1, we mentioned the connection between our method and the stochastic EM algorithm [Celeux and Diebolt, 1985]. The difference is in the M-step; to perform EM [Dempster *et al.*, 1977] we need only modify our sampler by: (a) sampling infinite branching structures at each iteration, and (b) re-calculating the probability of the branching structure with the M.A.P. μ and $\phi(\cdot)$, given the infinite set of branching structures. More specifically, maximizing the expected log posterior distribution to estimate M.A.P. μ and $\phi(\cdot)$ given infinite branching structures is equivalent to maximizing the EM objective in the M-step (see Appendix B for the formal derivation). Finally, note that the above step (b) is identical to the E-step of the EM algorithm.

EM-Hawkes. Following the discussion above, we propose *EM-Hawkes*, an approximate EM algorithm variant of Gibbs-Hawkes proposed in Section 3. Specifically, at each iteration EM-Hawkes (a) samples a finite number of cluster assignments (to approximate the expected log posterior distribution), and (b) finds the M.A.P. triggering kernels and background intensities rather than sampling them as per block Gibbs sampling (the M-step of the EM algorithm). An overview of the Gibbs-Hawkes, EM-Hawkes and EM algo-

Operation	Complexity
$p(\mu B)$	$O(1)$
p_{ij}	$O(N)$
$p(\phi B)$	$O((N_o + K)K^2)$
overall	$O((N + K)K^2)$

Table 2: Time Complexity.

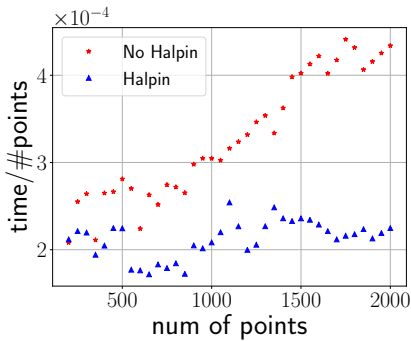


Figure 3: Computation time for calculating p_{ij} and sampling branching structures, with and without Halpin’s speed up.

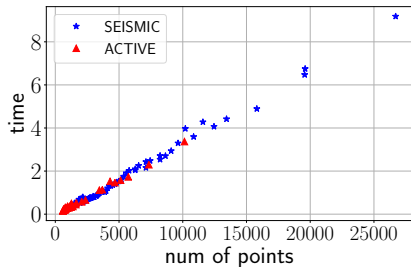


Figure 4: Running time per iteration on ACTIVE and SEISMIC.

rithm is illustrated in Fig. 2.

Note that under our LBPP-like posterior, finding the most likely triggering kernel $\phi(\cdot)$ is intractable (see Appendix C) As an approximation we take the element-wise mode of the *marginals* of the $\{\phi(t_i)\}_i$ to approximate the mode of the joint distribution of the $\{\phi(t_i)\}_i$.

5 Experiments

We now evaluate our proposed approaches — Gibbs-Hawkes and EM-Hawkes — and compare them to three baseline models, on synthetic data and on two large Twitter online diffusion datasets. The three baselines are: (1) A naive parametric Hawkes equipped with a constant background intensity and an exponential (Exp) triggering kernel $\phi = a_1 a_2 \exp(-a_2 t)$, $a_1, a_2 > 0$, estimated by maximum likelihood. (2) Ordinary differential equation (ODE)-based non-parametric non-bayesian Hawkes [Zhou *et al.*, 2013b]. (3) Wiener-Hopf (WH) equation based non-parametric non-bayesian Hawkes [Bacry and Muzy, 2014]. Codes of ODE based and WH based methods are publicly available [Bacry *et al.*, 2017].

5.1 Synthetic Data

We employ two toy Hawkes processes to generate data, both having the same background intensity $\mu = 10$, and cosine (Eq. (18)) and exponential (Eq. (19)) triggering kernels respectively. Note that compared to the cosine triggering kernel, the exponential one has a larger L2 norm for its derivative, and the difference is designed to test the performance of the approaches in different situations. We can check that both triggering kernels have negligible values when the input

Data	Exp	ODE	WH	Gibbs	EM
ϕ_{\cos}	0.661	0.553	1.000	0.338	0.318
μ_{\cos}	0.069	0.071	1.739	0.078	0.119
AVG_{\cos}	0.365	0.312	1.370	0.208	<u>0.219</u>
ϕ_{\exp}	0.120	0.610	1.000	0.147	<u>0.140</u>
μ_{\exp}	0.086	0.309	4.631	0.103	0.204
AVG_{\exp}	0.103	0.460	2.816	<u>0.125</u>	0.172
ACTIVE	2.369	2.370	1.315	<u>2.580</u>	2.592
SEISMIC	3.335	3.357	2.131	<u>3.576</u>	3.578

Table 3: Empirical performance comparison between algorithms (columns) with different measures (rows). *Top*: relative L2 distance to known ϕ and μ , and AVG denoted the average of L2 errors of ϕ and μ . *bottom*: mean predictive log likelihood on real data. Bold numbers denote the best performance and the underlined numbers for the second best.

is large in the domain which we will choose as $[0, \pi]$, so the finite support assumption is satisfied.

$$\phi_{\cos}(t) = \cos(3\pi t) + 1, \quad t \in (0, 1]; \quad 0, \quad \text{otherwise}; \quad (18)$$

$$\phi_{\exp}(t) = 5 \exp(-5t), \quad t > 0. \quad (19)$$

Prediction. For three baseline models and EM-Hawkes, the predictions μ_{pred} and $\phi_{\text{pred}}(\cdot)$ are taken to be the M.A.P. values, while for Gibbs-Hawkes we use the posterior mean.

Evaluation. Each toy model generates 400 point sequences over $\Omega = [0, \pi]$, which are evenly split into 40 groups, 20 for training and 20 for test. Each of the three methods fit on each group, *i.e.*, summing log-likelihoods for 10 sequences (for the parametric Hawkes) or estimating the log posterior probability of the Hawkes process given 10 sequences (for Gibbs-Hawkes and EM-Hawkes) or fitting the superposition of 10 sequences [Xu *et al.*, 2018]. Since the true models are known, we evaluate fitting results using the relative L2 distance between predicted and true μ and $\phi(\cdot)$: $d_{L2}(g_{\text{pred}}, g_{\text{true}}) = (\int_{\Omega} (g_{\text{pred}}(t) - g_{\text{true}}(t))^2 dt)^{1/2} / (\int_{\Omega} (g_{\text{true}}(t))^2 dt)^{1/2}$.

Experimental Details. For Gibbs-Hawkes and EM-Hawkes, we must select parameters of the GP kernel (Eqs. (12) to (14)). An arbitrary choice of them can lead to poor performance, and to this end, we apply the standard cross validation based on the log-likelihood. We choose the number of basis functions in $[8, 16, 32, 64, 128]$ and $a = b$ from $[0.2, 0.02, \dots, 2 \times 10^{-8}]$. We found that having many basis functions leads to a high fitting accuracy, but low speed. So, we use 32 basis functions which provides a suitable balance. In terms of kernel parameters a, b of Equation (13), we observed that large values return smooth triggering kernels which have a large distance to the ground truth, while small values result in non-smooth predictions which however have small log-likelihoods. As a result, the values $a, b = 0.002$ were chosen. 5000 iterations are run to fit each group and first 1000 are ignored (*i.e.* *burned-in*).

Results. The top of Table 3 shows the mean relative L2 distance between the learned and the true ϕ and μ on toy data. First, Gibbs-Hawkes and EM-Hawkes are the closest the models to the ground truth cosine model according to the

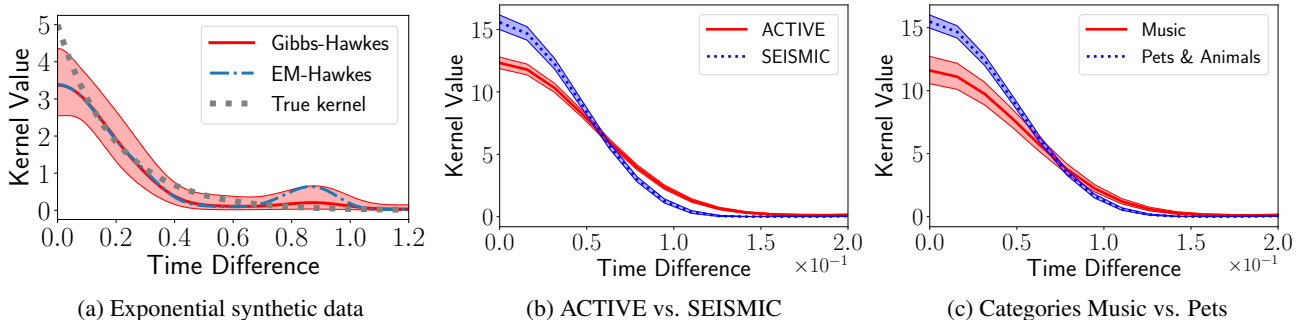


Figure 5: Learned Hawkes triggering kernels using our non-parametric Bayesian approaches. Each red or blue area shows the estimated posterior distributions of ϕ , while the solid lines indicate the 10, 50 and 90 percentiles. (a) A synthetic dataset simulated using $\phi_{\text{exp}}(t)$ (Eq. (19), shown in gray), is fit using Gibbs-Hawkes (in red) and EM-Hawkes (in blue); (b) Twitter data in ACTIVE (in red) and SEISMIC (in blue); (c) Twitter data associated with two categories in the ACTIVE set: Music (in red) and Pets & Animals (in blue).

average error values (AVG_{cos}). For the exponential simulation model, both approaches gain the second and the third lowest errors respectively among all methods, and as expected, the parametric Hawkes – which uses an exponential kernel – fits the model best. In contrast, the parametric model retrieves the cosine model worse because of its mismatch with the ground truth model. The learned triggering kernels for ϕ_{exp} and ϕ_{cos} by our approaches are shown in Fig. 5a and Fig. 6 in the appendix. The ODE-based method performs unsatisfactorily on both simulation settings and it is observed that it performs better on $(\mu_{\text{cos}}, \phi_{\text{cos}})$ than on $(\mu_{\text{exp}}, \phi_{\text{exp}})$. We explain the second observation as that the regularization of the ODE-based method encourages those triggering kernels that have small L2 norms for their derivatives and the derivative of $\phi_{\text{exp}}(x)$ has a larger norm than that of $\phi_{\text{cos}}(x)$. Notably, tuning the hyper-parameters of the WH method is challenging, and Table 3 shows the best result obtained after a rather exhaustive experimentation. We speculate that the overall better performance of our approaches is due to the regularization induced by the prior distributions and less difficult hyper-parameter selection. In addition, we also note that EM-Hawkes always performs better at discovering triggering kernels than Gibbs-Hawkes and this observation also holds on the real-life data. Thus, we conclude that generating multiple samples per iteration tends to improve modeling of the triggering kernels. In summary, compared with state-of-the-art methods, our approaches achieve better performances for data generated by kernels from several parametric classes; as expected, the parametric models are only effective for data generated from their own class.

Effect of Halpin’s Procedure. In Section 3.4, we show that using Halpin’s procedure reduces the complexity of calculating p_{ij} from quadratic to linear. We now empirically validate this speed up. To distinguish between quadratic and linear complexity, we compute the ratio between running time and data size, as shown in Fig. 3. The ratio when using Halpin’s procedure remains roughly constant as data size increases (the ratio increases linearly without the optimization), which implies that Halpin’s procedure renders linear calculation of p_{ij} and of branching structures. Later, we will show the linear

complexity of our method on real data.

5.2 Twitter Diffusion Data

We evaluate the performance of our two proposed approaches (Gibbs-Hawkes and EM-Hawkes) on two Twitter datasets, containing retweet cascades. A retweet cascade contains an original tweet, together with its direct and indirect retweets. Current state of the art diffusion modeling approaches [Zhao *et al.*, 2015; Mishra *et al.*, 2016; Rizoiu *et al.*, 2018] are based on the self-exciting assumption: users get in contact with on-line content, and then diffuse it to their friends, therefore generating a cascading effect. The two datasets we use have been employed in prior work and they are publicly available:

- ACTIVE [Rizoiu *et al.*, 2018] contains 41k retweet cascades, each containing at least 20 (re)tweets with links to Youtube videos. It was collected in 2014 and each Youtube video (and therefore each cascade) is associated with a Youtube category, e.g., *Music* or *News*.
- SEISMIC [Zhao *et al.*, 2015] contains 166k randomly sampled retweet cascades, collected in from Oct 7 to Nov 7, 2011. Each cascade contains at least 50 tweets.

Setup. The temporal extent of each cascade is scaled to $[0, \pi]$, and assigned to either training or test data with equal probability. We bundle together groups of 30 cascades of similar size, and we estimate one Hawkes process for each bundle. Unlike for the synthetic dataset, for the retweet cascades dataset there is no *true* Hawkes process to evaluate against. Instead, we measure using log-likelihood how well the learned model generalizes to the test set. We use the same hyper-parameters values as for the synthetic data. Finally, we follow the prior works on these cascade datasets [Zhao *et al.*, 2015; Rizoiu *et al.*, 2018] by setting the background intensity μ as 0, because the cascade datasets contain only the information of triggering relationships.

Fitting Performance. For each dataset, we calculate the log-likelihood per event for each tweet cascade obtained by three baselines and our approaches (Table 3). Visibly, our proposed methods consistently outperform baselines, with EM-Hawkes performing slightly better than Gibbs-Hawkes

(by 0.5% for ACTIVE and 0.06% for SEISMIC). This seems to indicate that online diffusion is influenced by factors not captured by the parametric kernel, therefore justifying the need to learn the Hawkes kernels non-parametrically. As mentioned in the synthetic data part, the WH-based method has a disadvantage of hard-to-tune hyper-parameters, which leads to the worst performance among all methods.

Scalability. To validate the linear complexity of our method, we record running time per iteration of Gibbs-Hawkes on ACTIVE and SEISMIC in Fig. 4. The running time rises linearly with the number of points increasing, in line with the theoretical analysis. Linear complexity makes our method scalable and applicable on large datasets.

Interpretation. We show in Fig. 5b and Fig. 5c the learned kernels for information diffusions. We notice that the learned kernels appear to be decaying and long-tailed, in accordance with the prior literature. Fig. 5b shows that the kernel learned on SEISMIC is decaying faster than the kernel learned on ACTIVE. This indicates that non-specific (i.e. random) cascades have a faster decay than video-related cascades, presumably due to the fact that Youtube videos stay longer in the human attention. This connection between the type of content and the speed of the decay seems further confirmed in Fig. 5c, where we show the learned kernels for two categories in ACTIVE: *Music* and *Pets & Animals*. Cascades relating to *Pets & Animals* have a faster decaying kernel than *Music*, most likely because Music is an ever-green content.

6 Conclusions

In this paper, we provided the first non-parametric Bayesian inference procedure for the Hawkes process which requires no discretization of the input domain and enjoys a linear time complexity. Our method iterates between two steps. First, it samples the branching structure, effectively transforming the Hawkes process into a cluster of Poisson processes. Next, it estimates the Hawkes triggering kernel using a non-parametric Bayesian estimation of the intensity of the cluster Poisson processes. We provide both a full posterior sampler and an EM estimation algorithm based on our ideas. We demonstrated our approach can infer flexible triggering kernels on simulated data. On two large Twitter diffusion datasets, our method outperforms the state-of-the-art in held-out likelihood. Moreover, the learned non-parametric kernel reflects the intuitive longevity of different types of content. The linear complexity of our approach is corroborated on both the synthetic and real problems. The present framework is limited to the univariate unmarked Hawkes process and will be extended to marked multivariate Hawkes process.

Acknowledgements

This research was supported in part by the Australian Government through the Australian Research Council’s Discovery Projects funding scheme (project DP180101985).

References

[Adams *et al.*, 2009] Ryan Prescott Adams, Iain Murray, and David J C MacKay. Tractable nonparametric bayesian in-

ference in poisson processes with gaussian process intensities. In *ICML*, pages 9–16, 2009.

- [Bacry and Muzy, 2014] Emmanuel Bacry and Jean-Francois Muzy. Second order statistics characterization of hawkes processes and non-parametric estimation. *arXiv preprint*, 2014.
- [Bacry *et al.*, 2017] Emmanuel Bacry, Martin Bompaire, Stéphane Gaïffas, and Soren Poulsen. tick: a python library for statistical learning, with a particular emphasis on time-dependent modeling. *ArXiv preprint*, 2017.
- [Celeux and Diebolt, 1985] Gilles Celeux and Jean Diebolt. The sem algorithm: A probabilistic teacher algorithm derived from the EM algorithm for the mixture problem. *Comp. Stat. Quarterly*, 2:73–82, 1985.
- [Dempster *et al.*, 1977] Arthur P Dempster, Nan M Laird, and Donald B Rubin. Maximum likelihood from incomplete data via the em algorithm. *Journal of the Royal Statistical Society, Series B*, 39(1):1–38, 1977.
- [Diggle *et al.*, 2013] Peter J Diggle, Paula Moraga, Barry Rowlingson, and Benjamin M Taylor. Spatial and spatio-temporal log-gaussian cox processes: extending the geostatistical paradigm. *Statistical Science*, 28(4):542–563, 2013.
- [Donnet *et al.*, 2018] Sophie Donnet, Vincent Rivoirard, and Judith Rousseau. Nonparametric bayesian estimation of multivariate hawkes processes. *arXiv preprint*, 2018.
- [Flaxman *et al.*, 2017] Seth Flaxman, Yee Whye Teh, and Dino Sejdinovic. Poisson intensity estimation with reproducing kernels. In *AISTATS*, pages 270–279, 2017.
- [Halpin, 2013] Peter F Halpin. A scalable em algorithm for hawkes processes. *New Developments in Quantitative Psychology*, pages 403–414, 2013.
- [Hawkes and Oakes, 1974] Alan Hawkes and David Oakes. A cluster process representation of a self-exciting process. *Journal of Applied Probability*, 11(3):493–503, 1974.
- [Hawkes, 1971] Alan Hawkes. Spectra of some self-exciting and mutually exciting point processes. *Biometrika*, 58(1):83–90, 1971.
- [Ishwaran and James, 2001] Hemant Ishwaran and Lancelot F James. Gibbs sampling methods for stick-breaking priors. *Journal of the American Statistical Association*, 96(453):161–173, 2001.
- [Kurashima *et al.*, 2018] Takeshi Kurashima, Tim Althoff, and Jure Leskovec. Modeling interdependent and periodic real-world action sequences. In *WWW*, pages 803–812, 2018.
- [Lewis and Mohler, 2011] Erik Lewis and George Mohler. A nonparametric em algorithm for multiscale hawkes processes. *Journal of Nonparametric Statistics*, 1(1):1–20, 2011.
- [Linderman and Adams, 2015] Scott W Linderman and Ryan P Adams. Scalable bayesian inference for excitatory point process networks. *arXiv preprint*, 2015.
- [Lloyd *et al.*, 2015] Chris Lloyd, Tom Gunter, Michael A Osborne, and Stephen J Roberts. Variational inference for gaussian process modulated poisson processes. In *ICML*, pages 1814–1822, 2015.

- [Mercer, 1909] James Mercer. Functions of positive and negative type, and their connection with the theory of integral equations. *Philosophical Transactions of the Royal Society A*, 209:415–446, 1909.
- [Mishra *et al.*, 2016] Swapnil Mishra, Marian-Andrei Rizoiu, and Lexing Xie. Feature driven and point process approaches for popularity prediction. *CIKM*, pages 1069–1078, 2016.
- [Møller *et al.*, 1998] Jesper Møller, Anne Randi Syversveen, and Rasmus Plenge Waagepetersen. Log gaussian cox processes. *Scandinavian journal of statistics*, 25(3):451–482, 1998.
- [Rasmussen and Williams, 2005] Carl Edward Rasmussen and Christopher K I Williams. *Gaussian Processes for Machine Learning*. The MIT Press, 2005.
- [Rasmussen, 2013] Jakob Gulddahl Rasmussen. Bayesian inference for hawkes processes. *Methodology and Computing in Applied Probability*, 15(3):623–642, 2013.
- [Rizoiu *et al.*, 2018] Marian-Andrei Rizoiu, Swapnil Mishra, Quyu Kong, Mark Carman, and Lexing Xie. Sirhawkes: Linking epidemic models and hawkes processes to model diffusions in finite populations. In *WWW*, pages 419–428, 2018.
- [Rubin, 1972] Izhak Rubin. Regular point processes and their detection. *IEEE Transactions on Information Theory*, 18(5):547–557, 1972.
- [Shirai and Takahashi, 2003] Tomoyuki Shirai and Yoichiro Takahashi. Random point fields associated with certain fredholm determinants ii: Fermion shifts and their ergodic and gibbs properties. *The Annals of Probability*, 31(3):1533–1564, 2003.
- [Walder and Bishop, 2017] Christian J Walder and Adrian N Bishop. Fast bayesian intensity estimation for the permanent process. In *ICML*, pages 3579–3588, 2017.
- [Xu *et al.*, 2016] Hongteng Xu, Mehrdad Farajtabar, and Hongyuan Zha. Learning granger causality for hawkes processes. In *ICML*, pages 1717–1726, 2016.
- [Xu *et al.*, 2018] Hongteng Xu, Dixin Luo, Xu Chen, and Lawrence Carin. Benefits from superposed hawkes processes. *AISTATS*, pages 623–631, 2018.
- [Zhao *et al.*, 2015] Qingyuan Zhao, Murat A Erdogdu, Hera Y He, Anand Rajaraman, and Jure Leskovec. Seismic: A self-exciting point process model for predicting tweet popularity. In *SIGKDD*, pages 1513–1522, 2015.
- [Zhou *et al.*, 2013a] Ke Zhou, Hongyuan Zha, and Le Song. Learning social infectivity in sparse low-rank networks using multi-dimensional hawkes processes. In *AISTATS*, pages 641–649, 2013.
- [Zhou *et al.*, 2013b] Ke Zhou, Hongyuan Zha, and Le Song. Learning triggering kernels for multi-dimensional hawkes processes. In *ICML*, pages III–1301–III–1309, 2013.

A Computing the Integral Term of the Log-likelihood

We consider $\Omega = [0, T]$, the background intensity μ , the triggering kernel $\phi(\cdot) = 1/2f(\cdot)^2$, $f(\cdot) = \boldsymbol{\omega}^T \mathbf{e}(\cdot)$, and data $\{t_i\}_{i=1}^N$, and the integral term in the log-likelihood is calculated as below

$$\begin{aligned}
 & \text{Integral Term} \\
 &= -\frac{1}{2} \sum_{i=1}^N \int_0^T f^2(t - t_i) dt \\
 &= -\frac{1}{2} \sum_{i=1}^N \int_0^{T-t_i} \left[\sum_{k=1}^K \omega_k e_k(t) \right]^2 dt \\
 &= -\frac{1}{2} \sum_{i=1}^N \sum_{k=1}^K \sum_{k'=1}^K \omega_k \omega_{k'} \underbrace{\int_0^{T-t_i} e_k(t) e_{k'}(t) dt}_{U_{kk'}^{(i)}} \\
 &= -\frac{1}{2} \sum_{i=1}^N \boldsymbol{\omega}^T U^{(i)} \boldsymbol{\omega}. \tag{20}
 \end{aligned}$$

In our case, Eq. (14) has $d = 1$, i.e., $\phi_k(x) = (2/\pi)^{1/2} \sqrt{1/2}^{[k-1=0]} \cos[(k-1)x]$, $k = 1, 2, \dots$. The matrix $U^{(i)}$ is calculated as below:

$$\begin{aligned}
 U_{1,1}^{(i)} &= \int_0^{T-t_i} \frac{1}{\pi} dt = \frac{T-t_i}{\pi}, \\
 U_{k>1,1}^{(i)} &= U_{1,k>1}^{(i)} = \frac{\sqrt{2} \sin[(k-1)(T-t_i)]}{\pi(k-1)}, \\
 U_{k,k(k>1)} &= \frac{1}{\pi} \left\{ T-t_i + \frac{\sin[2(k-1)(T-t_i)]}{2(k-1)} \right\}, \\
 U_{k,k'(k \neq k')} &= \frac{1}{\pi} \left\{ \frac{\sin[(k-k')(T-t_i)]}{k-k'} + \frac{\sin[(k+k'-2)(T-t_i)]}{k+k'-2} \right\}.
 \end{aligned}$$

B M.A.P. μ and ϕ Given Infinite Branching Structures

M.A.P. μ and ϕ given infinite branching structures is written as:

$$\begin{aligned}
 & \operatorname{argmax}_{\boldsymbol{\omega}, \mu} \mathbb{E}_B [\log p(\boldsymbol{\omega}, \mu | B, \{t_i\}_{i=1}^N, \Omega, k)] \\
 &= \operatorname{argmax}_{\boldsymbol{\omega}, \mu} \underbrace{\mathbb{E}_B [\log p(\{t_i\}_{i=1}^N | \boldsymbol{\omega}, \mu, B, \Omega, k)]}_{\text{Expected Log-likelihood}} + \underbrace{\log p(\boldsymbol{\omega}) + \log p(\mu)}_{\text{Constraints}} \\
 &= \operatorname{argmax}_{\boldsymbol{\omega}, \mu} \sum_{i=1}^N \left\{ \sum_{t_j < t_i} p_{ij} \log \frac{1}{2} [\boldsymbol{\omega}^T \mathbf{e}(t_i - t_j)]^2 - p_{i0} \log \mu - \frac{1}{2} \int_0^{T-t_i} [\boldsymbol{\omega}^T \mathbf{e}(t - t_i)]^2 dt \right\} - (\beta + 1) \mu T \\
 & \quad - \frac{1}{2} \boldsymbol{\omega}^T \Lambda^{-1} \boldsymbol{\omega} - (\alpha - 1) \log \mu, \tag{21}
 \end{aligned}$$

where B represents the branching structure, p_{ij} the probabilities of triggering relationships shown as Eq. (9) and Eq. (10), and α, β are parameters of the Gamma prior of μT . The second line is obtained using Bayes' rule, which shows M.A.P. μ and ϕ given infinite branching structures is equivalent to maximizing the constrained expected log-likelihood, i.e., the objective function for the M-step of the EM algorithm and the third line is an explicit expression of the second line.

C Mode-Finding the Triggering Kernel

Here we demonstrate in detail the computational challenges involved in finding the posterior mode with respect to the value of the triggering kernel at multiple point locations. Consider the triggering kernel $\phi(\cdot) = \frac{1}{2} f^2(\cdot)$ where $f(\cdot)$ is Gaussian process distributed. For a dataset $\{t_i\}_{i=1}^N$, $\mathbf{X} \equiv \{f(t_i)\}_{i=1}^N = \{X_i\}_{i=1}^N$ has a normal distribution, i.e., $\{f(t_i)\}_{i=1}^N \sim \mathcal{N}(\mathbf{m}, \boldsymbol{\Sigma})$ where \mathbf{m} and $\boldsymbol{\Sigma}$ are the mean and the covariance matrix. The distribution of $\mathbf{Y} \equiv \{\phi(t_i)\}_{i=1}^N = \{Y_i\}_{i=1}^N$ is derived as below where F

is the cumulative density function and f the probabilistic density function.

$$\begin{aligned}
F_{\mathbf{Y}}(\mathbf{y}) &= P(-\sqrt{2y_i} < X_i < \sqrt{2y_i}, i = 1, \dots, N) \\
&= \int_{-\sqrt{2y_1}}^{\sqrt{2y_1}} \dots \int_{-\sqrt{2y_N}}^{\sqrt{2y_N}} \frac{1}{\sqrt{(2\pi)^N \Sigma^{-1}}} \exp\left[-\frac{(\mathbf{X} - \mathbf{m})^T \Sigma^{-1} (\mathbf{X} - \mathbf{m})}{2}\right] dX_1 \dots dX_N, \\
f_{\mathbf{Y}}(\mathbf{y}) &= \frac{\partial^N}{\partial y_1 \dots \partial y_N} F_{\mathbf{Y}}(\mathbf{y}) \\
&= \frac{1}{\sqrt{(2\pi)^N \Sigma^{-1}}} \left(\prod_{i=1}^N \frac{1}{2\sqrt{2y_i}}\right) \sum_{\mathbf{X} \in \times_{i=1}^N \{\sqrt{2y_i}, -\sqrt{2y_i}\}} \exp\left[-\frac{(\mathbf{X} - \mathbf{m})^T \Sigma^{-1} (\mathbf{X} - \mathbf{m})}{2}\right], \tag{22}
\end{aligned}$$

where \times is the Cartesian product. There are 2^N summations of exponential functions, which is intractable.

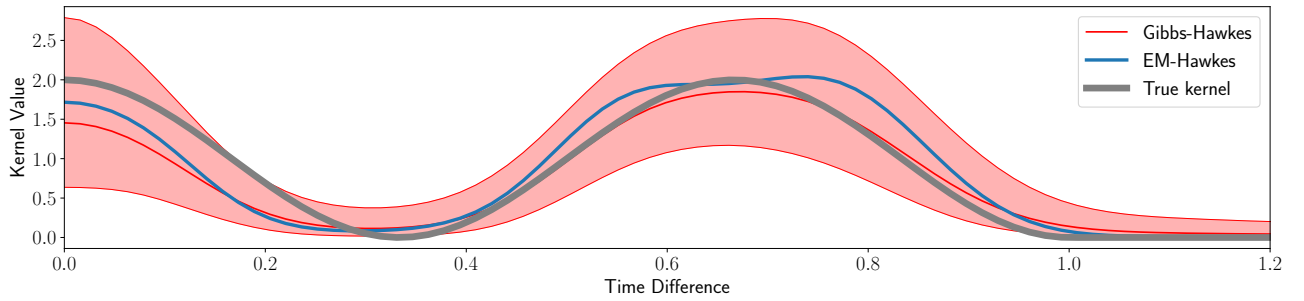


Figure 6: Triggering kernels estimated by the Gibbs-Hawkes method (Section 3) and the EM-Hawkes method (Section 4). The true kernel is plotted as the bold gray curve. We plot the median (red) and [0.1, 0.9] interval (filled red) of the approximate predictive distribution, along with the triggering kernel inferred by the EM Hawkes method (blue). The hyper-parameters a and b of the Gaussian process kernel (Eq. (13)) are set to 0.002.